Volume 4
Number 9
September 2017
Pages 1756-1912

Environmental Science
Nano

rsc.li/es-nano

USE PHASE

ISSN 2051-8153

ROYAL SOCIETY
OF CHEMISTRY

PAPER
Leanne M. Gilbertson et al
Methodology for quantifying engineered nanomaterial release
from diverse product matrices under outdoor weathering
conditions and implications for life cycle assessment

This is an Accepted Manuscript, which has been through the Royal Society of Chemistry peer review process and has been accepted for publication.

Accepted Manuscripts are published online shortly after acceptance, before technical editing, formatting and proof reading. Using this free service, authors can make their results available to the community, in citable form, before we publish the edited article. We will replace this Accepted Manuscript with the edited and formatted Advance Article as soon as it is available.

You can find more information about Accepted Manuscripts in the Information for Authors.

ROYAL SOCIETY
OF CHEMISTRY

rsc.li/es-nano

Environmental significance

Fluids in confined nanopores behave quite differently from the bulk ones, and the process is largely affected by the properties of flooding fluids. Due to dual characters of surface properties, Janus nanoparticles (NPs) possess great potential in tuning surface and interface properties compared to NPs with uniform surface properties. In our paper, the influence of Janus NPs on fluid flow properties in porous media is considered to study the flow mechanism. Understanding dynamics of fluids flow in confinement, especially nanopores in reservoirs, is crucial for the design of flooding fluids, which had significant implication to specific application fields such as enhanced oil recovery, groundwater remediation, water purification, CO_2 utilization, drug delivery, etc.

Transportation of Janus Nanoparticles in Confined Nanochannels: A Molecular Dynamics Simulations

Xiao Wang [1], Senbo Xiao [1], Zhiliang Zhang [1] and Jianying He [1,*]

[1] NTNU Nanomechanical Lab, Department of Structural Engineering, Faculty of Engineering, Norwegian University of Science and Technology (NTNU), 7491 Trondheim, Norway

Corresponding author:

Jianying He

Email: jianying.he@ntnu.no;

Tel.: +47-9380 4711

Abstract

Janus nanoparticles (JNPs) have drawn great attention due to their unique surface of dual characters. In this study, transportation of two-phase fluids with JNPs in an ultra-confined channel was studied by molecular dynamics (MD) simulations. The results indicated that the fluid displacement was hindered by JNPs, to an extent largely dependent on the concentration of NPs self-assembled at fluids interface. Different from NPs with uniform surface properties, the determining migration states for JNPs to influence displacement process were self-assembled at fluids interface and aggregated at three-phase contact region, which modified the interfacial tension and three-phase contact angle. Such key migration states were validated by the potential of mean force of JNPs transporting from water to oil phase. The capillary pressure calculated by local pressure distribution was found to be the key factor driving the displacement process of nanofluids with JNPs. Our findings revealed the microscopic transportation mechanism for fluids with JNPs into porous materials, which had significant implication to application fields such as enhanced oil recovery, drug delivery, inkjet printing, etc.

Keywords: Janus nanoparticles; Ultra-confined capillary; Two-phase displacement; Molecular dynamics simulation;

2

1. Introduction

Fluids flow dynamics in confined space is a fundamental research topic to oil recovery, [1] groundwater remediation, CO_2 utilization, and many others. [2-6] It is well known that behavior of fluids in confined channel has apparent difference compared to bulk systems. For instance, the viscosity of water-based fluids will decrease in hydrophobic nanochannels, and also largely depends on the size of the channel. [7, 8] The decreased viscosity can enhance the water transport velocity, beneficial to new material design for water desalination. [9] Apart from size effect of the channel, other key factors such as chemicals, wettability of channel, etc, [10, 11] can also be modified to form unique interaction between fluids and nanochannels, which is critical for designing new generation of fluids in targeted fields, particularly in enhanced oil recovery (EOR).

One of the important methods to modify the fluids properties in confined space is the addition of chemicals, such as surfactant, polymer, in the displacing phase. As previously reported, [12-15] nanoparticle (NP) has potential for tuning the viscosity of fluids, reducing interfacial tension, and altering the wettability of capillary, and thus modifying the displacement process of fluids in ultra-confined channel. The fluids properties are largely dependent on the properties of NPs like surface wettability, shape and size, concentration, etc. [16, 17]

In the past decades, Janus nanoparticles (JNPs) have received considerable attention due to their unique characteristic properties, namely the tailored opposite polarities on two distinct portions of NP surface. The JNP has great potential applications in the fields of biological, sensors, drug release, etc. [18-24] Experimentally, researchers usually adopted the phase separation method, self-assembly, and the sol-gel process to synthesize Janus emulsions. [25] Originated from the unique surface dual characters of JNPs and successful applications in other fields, a great deal of the researcher's attention have been attracted by the idea of employing JNPs in the field of oil recovery.

Researches on the Janus emulsions in water-oil interface have been well studied. [18] For instance, M. Wang et al. [24] studied the self-assembly behavior of gold JNPs at the water/oil interface and the influence of surface composition of JNPs at the water-oil interface. A. Striolo et al. [26-28] investigated the equilibrium behavior of JNPs at water-oil interface by dissipative particle dynamics (DPD) simulation. They concluded that the reduction of interfacial tension was closely related to the shape, adsorption orientation, and surface coverage with distribution of polar/nonpolar groups of JNPs. JNPs were found to be more efficient in reducing interfacial

tension than NPs with similar size, same composition and uniform surface properties[29]. However, most of investigations about JNPs focused on the reduction of interfacial tension, or the self-assembly morphologies in bulk phase. There are sparse studies concerning the behavior of JNPs in confined space. Meanwhile, due to the unique surface of dual characters in JNPs, the transportation mechanism of JNPs in confined nanochannel may differ from that of NPs with uniform surface properties. Understanding the displacement process of fluids transport controlled by JNPs remains unexplored and has great application in many fundamental fields.

Herein, all-atom molecular dynamic (MD) simulations were employed to study the influence of concentration of JNPs on water-oil flow in a confined cylindrical channel. By analyzing the motion behaviors of JNPs and relationship between displacement length (l) of nanofluids and time (t), the influence of NPs concentration on the fluid viscosity, interfacial tension, and capillary pressure were quantified to elucidate the displacement mechanism. Furthermore, the potential of mean force (PMF) for JNPs transporting from water phase to oil phase was calculated to evaluate the energy landscape of transportation in the confined channel. The local pressure distribution for fluids along the capillary was elaborated for understanding the dominating micro mechanism influenced by JNPs. Our results revealed the transportation mechanism of fluids with JNPs in the confined channel, shedding new light on the applications of JNPs.

2. Model and Simulation Details

The LAMMPS package [30] was employed to carry out MD simulations of nanofluids with JNPs transportation in the confined channel. A cylindrical capillary filled with oil molecules was constructed, followed by adding a box of nanofluid (water-based fluids with spherical JNPs) in the left side of the capillary. The capillary was built on face-centered cubic (FCC) crystal of silicon block with lattice constant 5.43 Å. The length of the silicon block was 194.1475 Å along y direction, and cross-section of the block was 65.1684 Å in both x and z directions in square shape. Atoms within radius of 25 Å in the center of the silicon blcok along the axial direction were removed to create the capillary space for transportation of nanofluids. The oil model consisted of 920 decane molecules in cylindrical shape within a radius of ~20 Å was built to fill the capillary as the displaced phase, as shown in Figure 1(a). The nanofluid consisted of 20,000 water molecules and spherical JNPs with a diameter of 7.0 Å (Figure 1(b)). The number of JNPs was varied with $N = 4$, 8 and 16 to investigate the effect of JNPs concentration. The NPs were placed in the water by removing the same volume of water molecules. A vacuum layer about 150 Å was placed at the exit of oil phase to supply sufficient

space to the displaced oil molecules.[4, 16] All the systems were conducted in a periodic orthorhombic box.

Figure 1

Atomistic parameters from the simple point charge/extend SPC/E model and CHARMM force field which have been widely used for water and oil molecules in many literatures, [31, 32] were employed for water and oil molecules, respectively. Standard pairwise 12-6 Lennard-Jones (L-J) potential was used for non-bonded intermolecular atom-atom interactions, and Lorentz-Berthelot mixing rule was used to combine the parameters for interactions between oil-water and oil-capillary with a cutoff distance of 1.0 nm. The particle–particle–particle–mesh (PPPM) algorithm with a convergence parameter of 10^{-4} was adopted to compensate the long range electrostatics interaction. [33] To enable spontaneous displacement process, the interaction of water with the inner surface of capillary must be stronger than that of oil molecules.[16] Interactions between capillary surface and water were unspecified and tuned by varying characteristic energy ε_{ij} in an appropriate range.[34, 35] Based on our previous simulations, [4] the value of 0.7 kcal/mol was chose to describe the interaction between water and capillary surface ε_{sw}, indicating a hydrophilic channel.

Four atomic interactions would affect the surface properties of NPs, including the interactions of NP-water ε_{nw}, NP-oil ε_{no}, NP-solid ε_{ns}, and NP-NP ε_{nn}. In the manner of previous studies, [17] the materials for special JNPs were not specified. In order to build JNPs, two different values of characteristic energy were designated to form JNPs with half hydrophobic and half hydrophilic properties. All the force field parameters were listed in Supporting Information Table S1.

MD simulations were carried out under the NVT ensemble (constant number of particles, volume, and temperature), with integrating the Newton's motion equation by Velocity Verlet algorithm. [36] The system temperature was controlled by Nosé–Hoover thermostat to keep constant value of 298K.[37] All the individual JNPs were treated as a single rigid entity without internal interaction, and the solid capillary was fixed in position to reduce simulation time. A simulation time of 16 ns with a timestep of 1.0 fs, which was needed for NP-free system to displace all oil molecules from capillary in a testing run, was applied to all systems for comparison. The obtained results were visualized by the VMD software.[38]

3. Results and Discussion

3.1 Spontaneous displacement process of nanofluids

The spontaneous displacement process of nanofluids in confined channel was monitored and shown in Figure 2. All the fluids entered into the capillary spontaneously and formed a concave meniscus with oil phase, indicating hydrophilic property of capillary. With increasing time, the concave meniscus of fluids moved along the capillary, and oil molecules were displaced out of the capillary. JNPs displayed three main behaviors, trapped at fluids interface, adsorbed onto the capillary and dispersed in water phase. In addition, there was one JNP transporting into oil phase for the cases of 4 JNPs and 16 JNPs in Figure 2. The number of JNPs in oil phase was very small and with the time increase , the JNPs transporting into oil phase tended to move back to fluid interface. Therefore, there were three main behaviors during whole displacement process. According to our previous reports,[4, 16] NPs tended to modify interfacial tension and fluids properties, significantly influencing the displacement process.

Figure 2

To further elucidate the displacement process, the relationship between displacement length (l) of nanofluid in capillary and time (t) was characterized in Figure 3(a). The distance from initial point to the location where local water density was 50% of its bulk value in confined channel was taken as the displacement length (l).[39, 40] From Figure 3(a), all the displacement curves showed the same trend. The major difference of displacement velocity occurred after 5.0 ns when the nanofluids had a steady flow state (Figure 3(b) and Figure 3(c)), showing a relative stable front of fluids interface and properties. The displacement curve for 4 JNPs fluid was almost indistinguishable from that of NP-free system, indicating little effect of JNPs at very low concentration on displacement process. When the number of added JNPs increased to 16, the displacement was slightly postponed. However, the displacement velocity for fluids with 8 JNPs had the smallest value, showing the slowest displacement compared with the other two systems of nanofluids. The retarded displacement mechanism by NP concentration will be further analyzed in the following text.

Figure 3

3.2 Fluids properties by JNPs in confined channel

It was revealed that the motion behavior of NPs in displacing fluid could alter the arrangement and orientation of fluids, modify the properties of fluids, and thus change displacement velocity. [41-44] Hydrophilic NPs tended to stick onto wall to alter wettability of the capillary, accelerating the displacement process, while hydrophobic NPs favored slipping along the capillary during displacement process.[16] As depicted in Figure 2, three main motion behaviors of JNPs were observed, namely dispersed in water phase, adsorbed onto solid wall,

and self-assembled at fluids interface. The number of NPs with different motion behaviors was counted in Table 1 to identify the role of JNPs in the displacement process.

At the beginning (2 ns), JNPs moved rapidly from the water phase to the fluid interface for all the systems. Such flow state was mostly driven by the Brownian dynamics of NPs and entropy. After 6 ns, the number of JNPs at fluid interface became relatively stable. For all the systems, NPs first dispersed in water phase, and gradually adsorbed on the capillary and self-assembled at fluids interface. The number of self-assembled NPs at fluids interface increased to a stable value if more JNPs added. Hence, it is important to identify the stable state for JNPs and the influence of different NP states on fluids properties in confined channel.

Table 1

3.2.1 JNPs self-assembled at the fluid interface

The NPs self-assembled at the fluid interface modify the interfacial tension. To assess that, the pressure difference between mean tangential stress tensors (i.e., Pxx and Pzz) and the normal one Pyy along the axial capillary was calculated in Figure 4. Here, all the systems after 8 ns were selected as the stable displacing state to calculate local pressure difference distribution along the capillary. To calculate local pressure difference, simulation box was divided into layers with the equal thickness along y direction. For different layer, the local pressure distribution was obtained by integrating the stress of atoms in each layer along tangential and normal directions. Four regions, namely bulk fluid, confined fluids, confined oil in capillary and bulk oil, were identified based on the pressure difference. The interfacial tension can be calculated by integrating the pressure difference curve along the capillary.[45] Herein, the total interfacial tension was the sum of tension for five interfaces of water-vacuum, water-solid, water-oil, oil-solid and oil-vacuum. Among others, the JNPs self-assembled at the fluid interface only alter the water-oil interfacial tension.

Figure 4

The total interfacial tension was calculated as 160.3 mN/m for NP-free system, 164.4 mN/m for N=4, 126.1 mN/m for N=8, and 125.4 mN/m for N=16, respectively. It indicated that the addition of low concentration JNPs had negligible effect on the interfacial tension. While for systems of N=8 and N=16, the interfacial tension was reduced to almost same value, owing to same number of NPs self-assembled at fluids interface at 8 ns. It was known that the reducing interfacial tension resulted in slower fluid displacement by Lucas–Washburn equation,[44] agreeing with the simulated conclusion that the displacement for fluids with N=8 and N=16 NPs was lower than that of N=0 and N=4.

Even though the interfacial tension was nearly identical for fluids with N=8 and N=16, the displacement for N=16 was slightly faster than the one with 8 JNPs. In order to clarify that, the water-oil interface for system with 16 JNPs was scrutinized in detail, as shown in Figure 5. Because of the crowded number of the NPs, they not only stayed at the fluid interface, but also aggregated at three-phase contact region of water, oil and solid, and moved together in a packed cluster along the three-phase contact line. These self-assembled JNPs influenced three-phase contact angle in confined channel, and contact angle was thus calculated to quantify the effect of JNPs. To determine contact angle, liquid in the capillary was firstly divided into cylindrical shells, and then subdivided by a thickness of 1.5 Å along axial direction. The meniscus curve of fluid-fluid interface was drawn according to the density of fluids in each shell, and the contact angle was obtained by fitting the density profiles.[16, 43, 46] For base fluids without NPs, the contact angle was about 28.5°. For fluids with JNPs, the angle with more NPs was labeled as θ_1, the less was treated as θ_2, as marked in Figure 5(b). The calculated angles were about 72.9° for θ_1 and 58.01° for θ_2, respectively, and both were much larger than that of the NP-free case. As indicated by former studies, contact angle had an inverse relationship with displacement length in capillary.[44] Here, the aggregated JNPs at three-phase contact region increased the contact angle, and resulted in decreased displacement.

Figure 5

According to the above analysis, JNPs self-assembled at fluids interface and at three-phase contact region reduced fluids interfacial tension and increased three-phase contact angle. Both contributed to the retarded displacement process.

3.2.2 JNPs adsorbed onto solid capillary

One of adsorbed JNPs was selected from system with 16 JNPs, and its position along the axial and radial direction was recorded during the following 2.0 ns to study the motion behavior, shown in Figure 6(a). It can be seen that the center of the JNP kept stable along radial direction, while the value along the axial direction had slight fluctuation, owing to the orientation and position adjusting of the Janus NP on the capillary wall. It indicated relatively stable state of JNPs onto the capillary with increased time, showing 'Sticking' behavior.[15]

Figure 6

To further validate the effect of adsorbed JNPs, simulation with lower interaction between NPs and solid capillary (ε_{ns} =0.2 kcal/mol) was performed. The resulted displacement process was shown in Figure 6 (b). There existed a competitive adsorption between JNPs and water molecules onto the capillary. After 16.0 ns, there was no oil phase left in the capillary

8

for two systems. The displacement velocity of nanofluids in solid channel with $\varepsilon_{ns}=0.2$ kcal/mol

was comparable to that of the other system (displacement curves shown in Section S2 of

Supporting Information). This can be ascribed to only one or two adsorbed JNPs onto solid

capillary (Table 1), which had a negligible influence on the displacement process.

3.2.3 JNPs dispersed into water phase

The dispersed particles in fluid phase caused rearrangement of water molecules, thus

influencing viscosity of fluids. The radial pair distribution function (RPF) $g(r)$ between the

center of JNP and oxygen in water was calculated in Figure 7(a). Furthermore, the density of

water around JNP was calculated in Figure S2 (Supporting Information). These results clearly

showed there was a water layer on the surface of JNP. However, compared with relative curves

of hydrophilic NP in our previous work,[16] the first peak density value and $g(r)$ were much

lower, indicating weaker interactions between the JNPs and the water molecules. This may

cause rapid exchange of water molecules in the first layer with the bulk water, and influence

water diffusion and viscosity of fluids.

Figure 7

Mean square displacement (MSD) was calculated to assess the diffusion property of

nanofluids in the confined channel, as shown in Figure 7(b). By linear fitting the MSD curve,

the diffusion coefficient for water molecules in confined channel was obtained as 2.26×10^{-9}

m^2/s,[47] and the calculated viscosity was 1.14 MPa·s at 298.15 K using Einstein relation,[4, 48]

which was slightly higher than bulk value due to the confinement effect. Meanwhile, there was

no distinct difference on MSD curves between NP-free case and nanofluids with varied

concentrations. The results suggested that the particles dispersed in water phase also had a

negligible influence on the displacement process.

The above analyses confirmed that the JNPs self-assembled at fluids interface or at three-

phase contact region is the dominating factor in the displacement process, while those adsorbed

onto capillary or dispersed in liquid phase has no significant effect on modifying the properties

of capillary or fluids.

3.3 Fluid displacement mechanism by JNPs

The potential of mean force (PMF) for JNPs migrating from water to oil phase in the

nanochannel illustrates the energy landscape of the JNPs' distribution in the confined channel,

which can shed light on the intrinsic mechanism of spontaneous displacement process and

provide essential theoretical guidelines for nanoparticle design.[46] Furthermore, capillary

9

pressure is critical to study the influence of JNPs in the displacement process.[16] Therefore, PMF and capillary pressure were assessed to disclose the displacement mechanism by JNPs.

3.3.1 Potential of mean force for JNPs transportation in confined channel

Due to the spontaneous displacement of nanofluids, JNPs migrated with the base fluid, and thus it was difficult to identify the energy landscape of NPs migration pathway in semi-equilibrium states. To quantify the energy differences between transportation states of Janus NPs in confined channel, PMF for JNP transporting in confined channel was calculated by umbrella sampling method.[49] In order to perform umbrella sampling, a series of configurations were generated along the reaction coordinate ξ, namely along the migration pathway of JNPs from the water to the oil phase. Firstly, the sampling windows of defined distance along the pathway were selected. Two neighbor windows overlapped at the edge to ensure the smoothness of the calculated PMF. All the windows sufficiently covered the whole pathway. The pulled group, the center of one JNP, was maintained initially at the center of each window by a biased potential, and to sample simulations in each window. The collected positions distribution of the pulled group in each window was then used for constructing the PMF profile by the WHAM method.[49, 50] The histograms of the configurations within umbrella sampling windows were given in Figure S3 (Supporting Information). The histograms showed sufficient overlapping between windows of the center of mass spacing, indicating the properly sampled reaction coordinate.

Figure 8

The PMF profile of JNP migration pathway was shown in Figure 8. It indicated that JNPs transportation along the capillary had local minimized energy and platform region. Combining with transportation snapshots, the local minimized energies occurred in the positions where JNPs attached onto capillary, moved along water-oil interface, and self-assembled at three-phase contact region. Analysis based on PMF profile drew the same conclusions with above discussions that the relative states for JNPs transportation in confined channel were self-assembled at fluids interface and three-phase contact region, which led to retarded displacement process.

3.3.2 Capillary pressure for fluids in confined capillary

Intrinsically, the addition of JNPs in water phase changes the pressure distribution of fluids, and thus modifies the capillary force and the viscous force, resulting in varied displacement velocity and efficiency. The local pressure distribution for fluids along capillary was characterized to clarify the influence of JNPs on displacement process (Supporting

Information S4). According to local pressure, the influence of JNPs on capillary pressure of fluids could be calculated by integrated the pressure for different fluids. The calculated capillary pressure for four systems was shown in Figure 9.

Figure 9

For NPs-free case, the calculated capillary pressure was 118.74 atm, while 83.66 atm for N=4, 24.04 atm for N=8 and 63.78 atm for N=16 JNPs, respectively. As discussed above, the reduction of interfacial tension for fluids with N=16 and N=8 were almost same. The main difference between these two systems was originated from three-phase contact angle according to Young-Laplace equation. For fluids with 16 JNPs, three NPs stayed at the three-phase contact line, and two at the fluid interface. According to studies by Wasan and Nikolov,[51] the NPs self-assembled at three-phase contact region could produce a structural disjoining pressure to promote the detachment of oil droplets from the solid surface. The reduced capillary pressure resulted in the decreased displacement velocity in the confined channel. Therefore, analysis of capillary pressure suggests the same tendency of the displacement process shown in Figure 3.

4. Conclusion

The transportation process for nanofluids with Janus nanoparticles (JNPs) in a confined cylindrical channel was studied by molecular dynamics simulations. The results indicated that JNPs hindered the displacement of nanofluids in the confined channel and their concentration significantly influenced the displacement process. The motion behaviors of JNPs had obvious effect on the dynamic properties of confined nanofluids. Especially, JNPs self-assembled at fluids interface could reduce the fluids interfacial tension, while the adsorbed JNPs on capillary or dispersed NPs in water phase had little influence on displacement process. The potential of mean force of JNP on its migration pathway also validated the important relative states for JNP in confined channel, namely adsorbed on capillary, fluids interface and three-phase contact region. The influence of JNPs concentration on displacement process was closely related to the number of JNPs at fluids interface and three-phase contact region. Meanwhile, the calculated capillary pressure suggested the same trend of displacement profiles, indicating the key factor in the displacement process by JNPs. Our findings revealed microscopic mechanism of two-phase fluids flow with JNPs into porous materials (such as polymers, or reservoir), which had great potential in the design of nanofluid and tunable properties in engineering and biomedicine fields, such as enhanced oil recovery, microfluidic devices, controlled drug release, inkjet printing, etc.

Supplementary Materials: The following are available online at http://.

Conflicts of Interest: The authors declare no conflict of interest.

References

1.   J. M. Berlin, J. Yu, W. Lu, E. E. Walsh, L. Zhang, P. Zhang, W. Chen, A. T. Kan, M. S. Wong, M. B. Tomson and J. M. Tour, Engineered nanoparticles for hydrocarbon detection in oil-field rocks, *Energy Environ. Sci.*, 2011, **4**, 505-509.

2.   J. M. de Almeida and C. R. Miranda, Improved oil recovery in nanopores: NanoIOR, *Sci. Rep.*, 2016, **6**, 28128.

3.   A. Bera and H. Belhaj, Application of nanotechnology by means of nanoparticles and nanodispersions in oil recovery - A comprehensive review, *J. Nat. Gas. Sci. Eng.*, 2016, **34**, 1284-1309.

4.   X. Wang, Z. Zhang, O. Torsaeter and J. He, Atomistic insights into the nanofluid transport through an ultra-confined capillary, *Phys. Chem. Chem. Phys.*, 2018, **20**, 4831-4839.

5.   Y. Lin, H. Skaff, T. Emrick, A. D. Dinsmore and T. P. Russell, Nanoparticle assembly and transport at liquid-liquid interfaces, *Science*, 2003, **299**, 226-229.

6.   Matthew K. Borg, Duncan A. Lockerby, Konstantinos Ritos and J. M. Reese, Multiscale simulation of water flow through laboratory-scale nanotube membranes, *J. Membrane. Sci.,* 2018, **567**, 115-126.

7.   J. A. Thomas and A. J. H. McGaughey, Reassessing Fast Water Transport Through Carbon Nanotubes, *Nano Lett*, 2008, **8**, 2788-2793.

8.   K. Wu, Z. Chen, J. Li, X. Li, J. Xua and X. Dong, Wettability effect on nanoconfined water flow, *Proc. Nat. Acad. Sci. U.S.A.*, 2017, **114**, 3358-3363.

9.   K. Yang, J. Wang, X. Chen, Q. Zhao, A. Ghaffar and B. Chen, Application of graphene-based materials in water purification: from the nanoscale to specific devices, *Environ. Sci.: Nano*, 2018, **5**, 1264-1297.

10.   C. Li, Y. Shen, H. Ge, Y. Zhang and T. Liu, Spontaneous imbibition in fractal tortuous micro-nano pores considering dynamic contact angle and slip effect: phase portrait analysis and analytical solutions, *Sci Rep*, 2018, **8**, 3919.

11.   J. Tang, Z. Qu, J. Luo, L. He, P. Wang, P. Zhang, X. Tang, Y. Pei, B. Ding, B. Peng and Y. Huang, Molecular Dynamics Simulations of the Oil-Detachment from the Hydroxylated Silica Surface: Effects of Surfactants, Electrostatic Interactions, and Water Flows on the Water Molecular Channel Formation, *J. Phys. Chem. B*, 2018, **122**, 1905-1918.

12.   Z. Hu, S. M. Azmi, G. Raza, P. W. J. Glover and D. Wen, Nanoparticle-Assisted Water-Flooding in Berea Sandstones, *Energy Fuels*, 2016, **30**, 2791-2804.

13.   E. A. Taborda, C. A. Franco, M. A. Ruiz, V. Alvarado and F. B. Cortés, Experimental and Theoretical Study of Viscosity Reduction in Heavy Crude Oils by Addition of Nanoparticles, *Energy Fuels*, 2017, **31**, 1329-1338.

14.   X. Wang, S. Xiao, Z. Zhang and J. He, Displacement of nanofluids in silica nanopores: influenced by wettability of nanoparticles and oil components, *Environ. Sci.: Nano*, 2018, **5**, 2641-2650.

15.   Y. Li, H. Wu and F. Wang, Effect of a Single Nanoparticle on the Contact Line Motion, *Langmuir*, 2016, **32**, 12676-12685.

16.   X. Wang, S. Xiao, Z. Zhang and J. He, Effect of Nanoparticles on Spontaneous Imbibition of Water into Ultraconfined Reservoir Capillary by Molecular Dynamics Simulation, *Energies*, 2017, **10**, 506.

17.   Y. Li, F. Wang, H. Liu and H. Wu, Nanoparticle-tuned spreading behavior of nanofluid droplets on the solid substrate, *Microfluidics and Nanofluidics*, 2014, **18**, 111-120.

18.   D. Luo, F. Wang, J. Zhu, F. Cao, Y. Liu, X. Li, R. C. Willson, Z. Yang, C. W. Chu and Z. Ren, Nanofluid of graphene-based amphiphilic Janus nanosheets for tertiary or enhanced oil recovery: High performance at low concentration, *Proc. Nat. Acad. Sci. U.S.A.*, 2016, **113**, 7711-7716.

19.   H. Fan, D. E. Resasco and A. Striolo, Amphiphilic silica nanoparticles at the decane-water interface: insights from atomistic simulations, *Langmuir*, 2011, **27**, 5264-5274.

20.   Y. Kobayashi and N. Arai, Self-Assembly and Viscosity Behavior of Janus Nanoparticles in Nanotube Flow, *Langmuir*, 2017, **33**, 736-743.

21.   A. Walther and A. H. Muller, Janus particles: synthesis, self-assembly, physical properties, and applications, *Chem Rev*, 2013, **113**, 5194-5261.

22.   J. Tang, P. J. Quinlan and K. C. Tam, Stimuli-responsive Pickering emulsions: recent advances and potential applications, *Soft Matter*, 2015, **11**, 3512-3529.

23.   P. Bayati and A. Najafi, Dynamics of two interacting active Janus particles, *J. Chem. Phys.*, 2016, **144**, 134901.

24.   M. Wang, Z. Zhang and J. He, A SERS Study on the Assembly Behavior of Gold Nanoparticles at the Oil/Water Interface, *Langmuir*, 2015, **31**, 12911-12919.

25.   X. H. Ge, J. P. Huang, J. H. Xu, J. Chen and G. S. Luo, Water-oil Janus emulsions: microfluidic synthesis and morphology design, *Soft Matter*, 2016, **12**, 3425-3430.

26.   H. Fan and A. Striolo, Nanoparticle effects on the water-oil interfacial tension, *Physical Review E*, 2012, **86**, 051610.

27.   X. C. Luu, J. Yu and A. Striolo, Ellipsoidal janus nanoparticles adsorbed at the water-oil interface: some evidence of emergent behavior, *J. Phys. Chem. B.*, 2013, **117**, 13922-13929.

28.   X. C. Luu and A. Striolo, Ellipsoidal Janus nanoparticles assembled at spherical oil/water interfaces, *J. Phys. Chem. B.*, 2014, **118**, 13737-13743.

29.   S. Drexler, J. Faria, M. P. Ruiz, J. H. Harwell and D. E. Resasco, Amphiphilic Nanohybrid Catalysts for Reactions at the Water/Oil Interface in Subsurface Reservoirs, *Energy Fuels*, 2012, **26**, 2231-2241.

30.   S. Plimpton, Fast Parallel Algorithms for Short-Range Molecular Dynamics, *J. Comput. Phys.*, 1995, **117**, 1-19.

31.   K. Vanommeslaeghe, E. Hatcher, C. Acharya, S. Kundu, S. Zhong, J. Shim, E. Darian, O. Guvench, P. Lopes, I. Vorobyov and A. D. Mackerell, Jr., CHARMM general force field: A force field

for drug-like molecules compatible with the CHARMM all-atom additive biological force fields, *J. Comput. Chem.*, 2010, **31**, 671-690.

32.   V. Zoete, M. A. Cuendet, A. Grosdidier and O. Michielin, SwissParam: a fast force field generation tool for small organic molecules, *J. Comput. Chem.*, 2011, **32**, 2359-2368.

33.   T. Darden, D. York and L. Pedersen, Particle mesh Ewald: An N·log(N) method for Ewald sums in large systems, *J. Chem. Phys.*, 1993, **98**, 10089-10092.

34.   S. Xiao, J. He and Z. Zhang, Nanoscale deicing by molecular dynamics simulation, *Nanoscale*, 2016, **8**, 14625-14632.

35.   S. Xiao, Z. Zhang and J. He, Atomistic dewetting mechanics of Wenzel and monostable Cassie-Baxter states, *Phys. Chem. Chem. Phys.*, 2018, **20**, 24759-24767.

36.   S. Nosé, A molecular dynamics method for simulations in the canonical ensemble, *Mol. Phys.*, 1984, **52**, 255-268.

37.   H. J. C. Berendsen, J. P. M. Postma, W. F. van Gunsteren, A. DiNola and J. R. Haak, Molecular dynamics with coupling to an external bath, *J. Chem. Phys.*, 1984, **81**, 3684-3690.

38.   W. Humphrey, A. Dalke and K. Schulten, VMD: Visual molecular dynamics, *J. Mol. Graph.*, 1996, **14**, 33-38.

39.   S. Supple and N. Quirke, Molecular dynamics of transient oil flows in nanopores. II. Density profiles and molecular structure for decane in carbon nanotubes, *J. Chem. Phys.*, 2005, **122**, 104706.

40.   M. Sedghi, M. Piri and L. Goual, Molecular dynamics of wetting layer formation and forced water invasion in angular nanopores with mixed wettability, *J Chem Phys*, 2014, **141**, 194703.

41.   J. Wu, J. He, O. Torsæter and Z. Zhang, Effect of Nanoparticles on Oil-Water Flow in a Confined Nanochannel: a Molecular Dynamics Study, 2012, SPE 156995.

42.   U. Anand, J. Lu, D. Loh, Z. Aabdin and U. Mirsaidov, Hydration Layer-Mediated Pairwise Interaction of Nanoparticles, *Nano Lett.*, 2016, **16**, 786-790.

43.   G. Martic, F. Gentner, D. Seveno, D. Coulon and J. D. Coninck, A Molecular Dynamics Simulation of Capillary Imbibition, *Langmuir*, 2002, **18**, 7971-7976.

44.   A. Hamraoui and T. Nylander, Analytical approach for the Lucas-Washburn equation, *J Colloid Interface Sci*, 2002, **250**, 415-421.

45.   J. Alejandre, D. J. Tildesley and G. A. Chapela, Molecular dynamics simulation of the orthobaric densities and surface tension of water, *J. Chem. Phys.*, 1995, **102**, 4574-4583.

46.   C. Chen, K. Lu, L. Zhuang, X. Li, J. Dong and J. Lu, Effective fluid front of the moving meniscus in capillary, *Langmuir*, 2013, **29**, 3269-3273.

47.   Y. Yan, X. Wang, Y. Zhang, P. Wang, X. Cao and J. Zhang, Molecular dynamics simulation of corrosive species diffusion in imidazoline inhibitor films with different alkyl chain length, *Corros. Sci.*, 2013, **73**, 123-129.

15

48.   N. Ohtori and Y. Ishii, Explicit expressions of self-diffusion coefficient, shear viscosity, and the Stokes-Einstein relation for binary mixtures of Lennard-Jones liquids, *J. Chem. Phys.*, 2015, **143**, 164514.

49.   Shankar Kumar, Djamal Bouzida, Robert H. Swendsen, Peter A. Kollman and J. M. Rosenberg, The Weighted Histogram Analysis Method for Free-Energy Calculations on Biomolecules. I. The Method, *J. Comput. Chem.*, 1992, **13**, 1011-1021.

50.   H. Yan and S. Yuan, Molecular Dynamics Simulation of the Oil Detachment Process within Silica Nanopores, *J. Phys. Chem. C.*, 2016, **120**, 2667-2674.

51.   A. D. N. Darsh T. Wasan, Spreading of nanofluids on solids, *Nature*, 2003, **423**, 156-159.

Figures
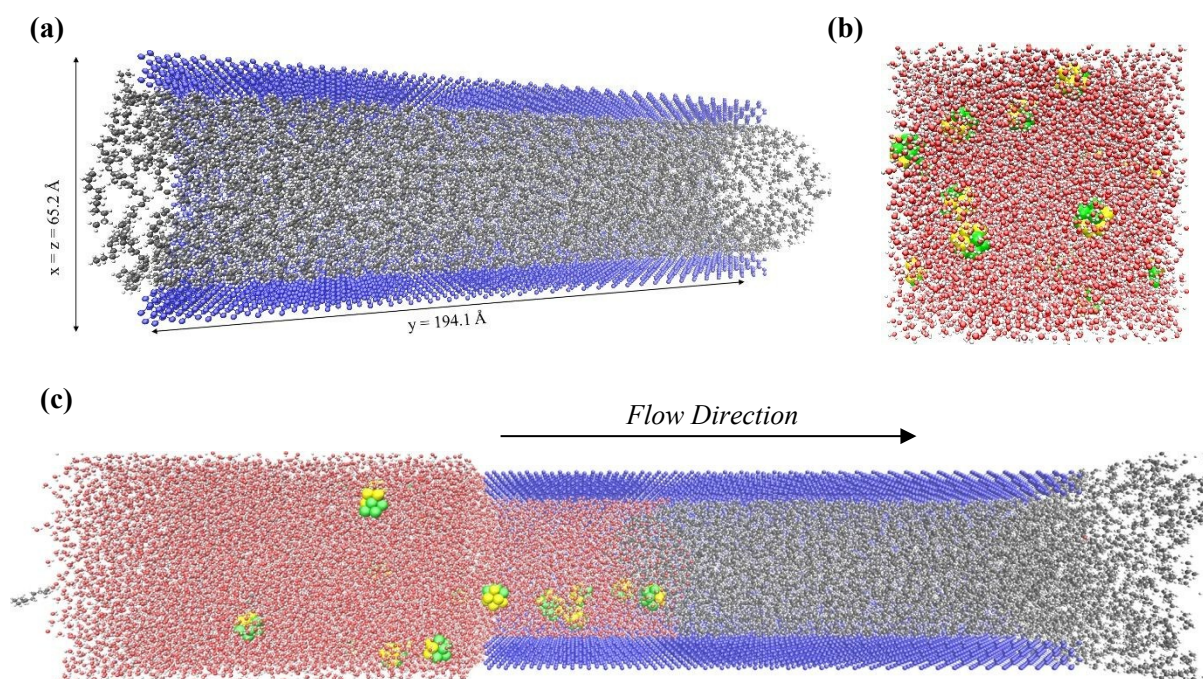
Figure 1 Atomistic models: (a) oil molecules in confined cylindrical capillary; (b) nanofluid with JNPs; (c) The schematic simulation system. The colors for different atoms: oxygen (red), hydrogen (white), capillary (blue), carbon (gray); hydrophilic part of JNP (green) and hydrophobic part of JNP (yellow).
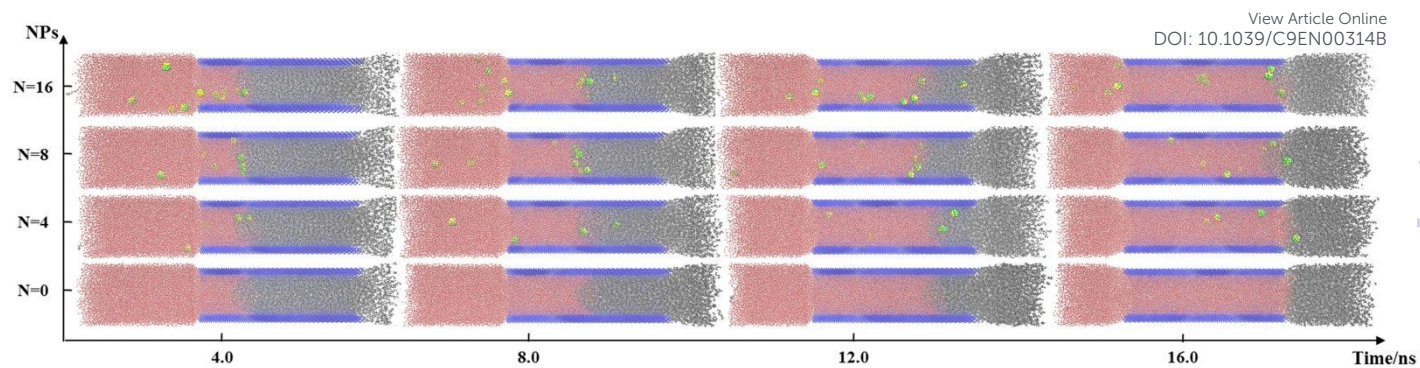
17

Figure 2 Displacement process of nanofluids in confined cylindrical capillary. The atoms share the same colors as those in Figure 1.
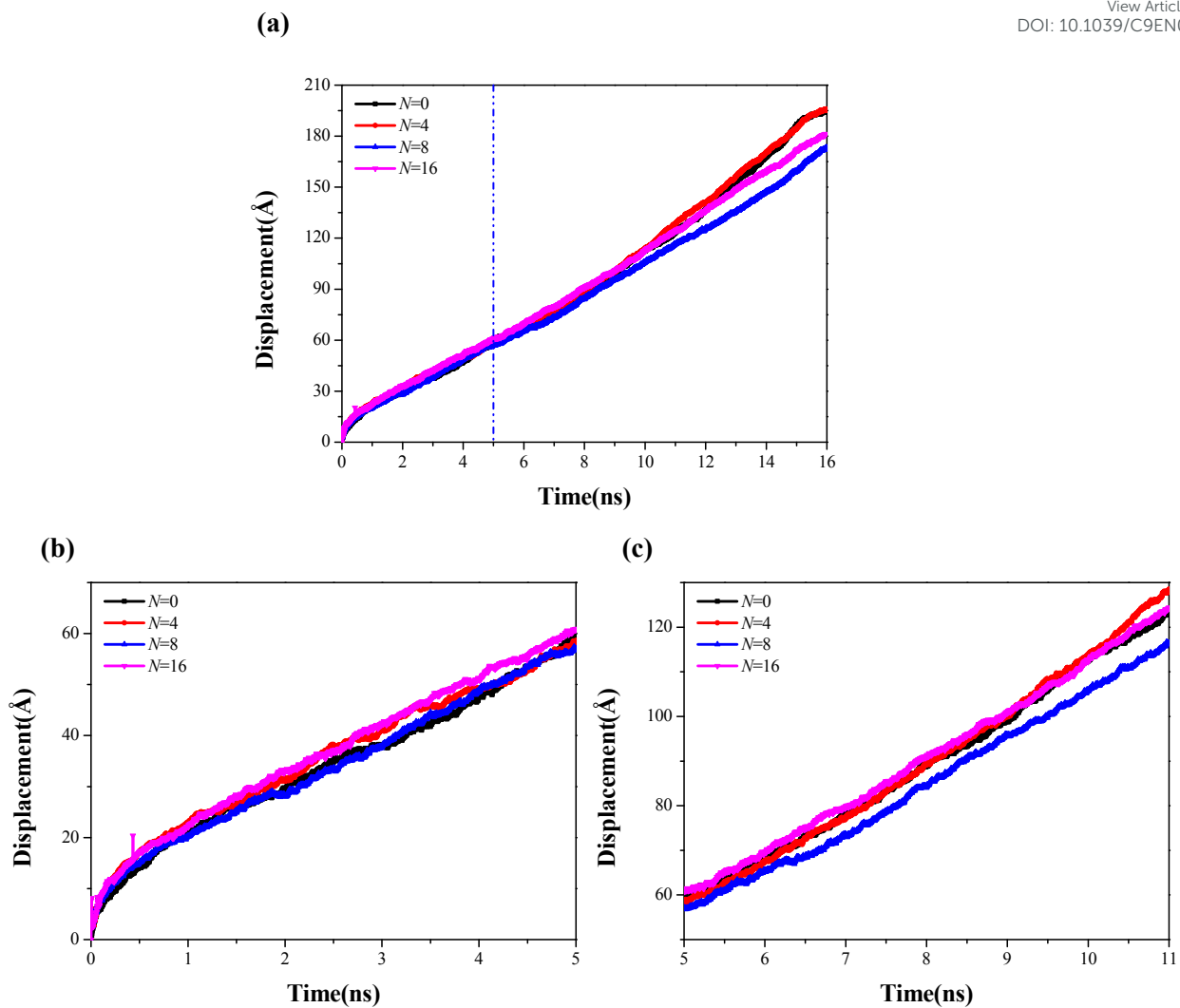
Figure 3 (a) The displacement of nanofluids with different concentration of JNPs; (b) enlarged displacement of nanofluids from 0.0 ns to 5.0 ns; (c) enlarged displacement of nanofluids from 5.0 ns to 11.0 ns

19

Table 1 Motion behaviors of JNPs in the systems.

Time(ns)	4 JNPs			8 JNPs			16 JNPs		
	Disperse	Adsorb	Interface	Disperse	Adsorb	Interface	Disperse	Adsorb	Interface
2	2	0	2	3	0	3	15	0	1
4	2	0	1	4	0	4	13	1	2
6	1	1	1	3	0	5	9	1	5
8	1	1	1	2	1	5	9	1	5
10	2	0	1	2	1	5	9	1	5
12	1	1	2	2	1	5	8	2	5
14	0	2	2	2	2	4	8	2	6

20
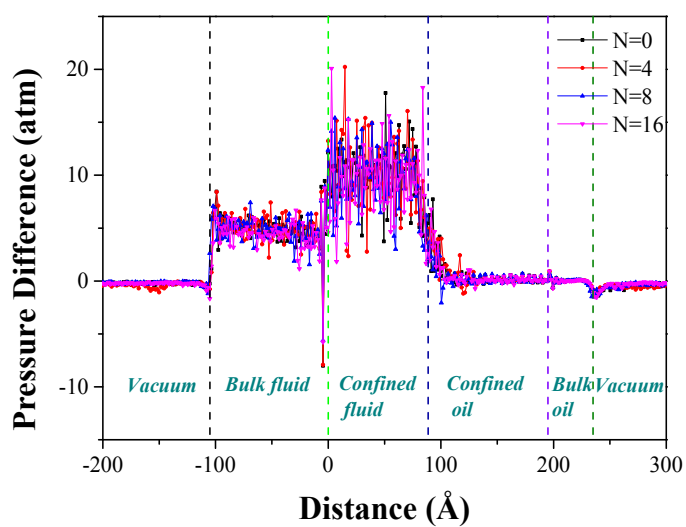
Figure 4 Pressure difference along the axial direction of the capillary.
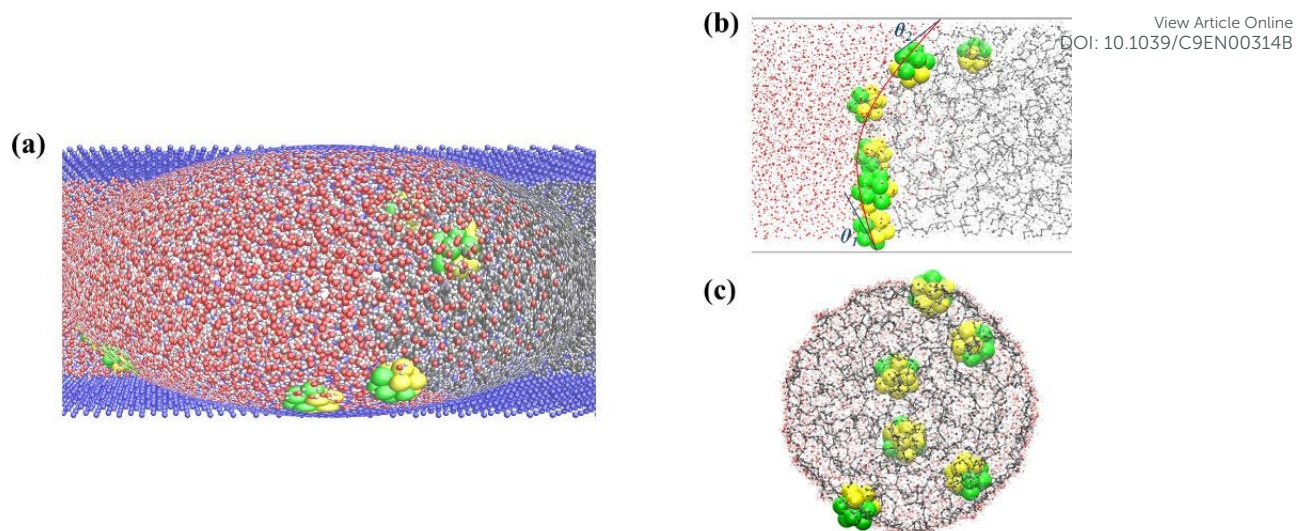
Figure 5 Configurations of JNPs at fluids interface: (a) the fluids in confined channel with enlarging interface region; (b) fluids interface from axial direction; (c) fluids interface from radial direction.

(a)

(b)
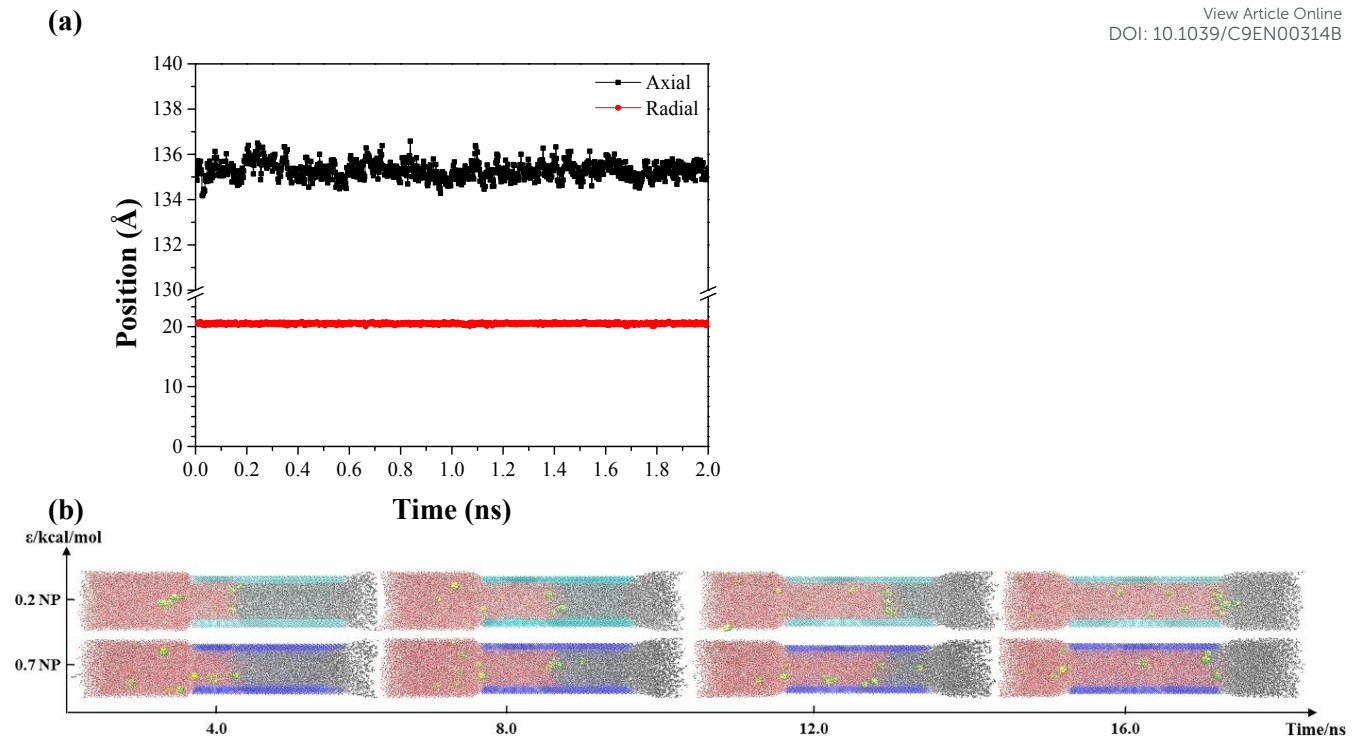
Figure 6 (a) The position of the adsorbed JNP in the axial and radial direction; (b) displacement process for nanofluids with different interaction between JNP and solid capillary. The capillary with low adsorption capacity is shown in cyan, and others are the same as in Figure 1.
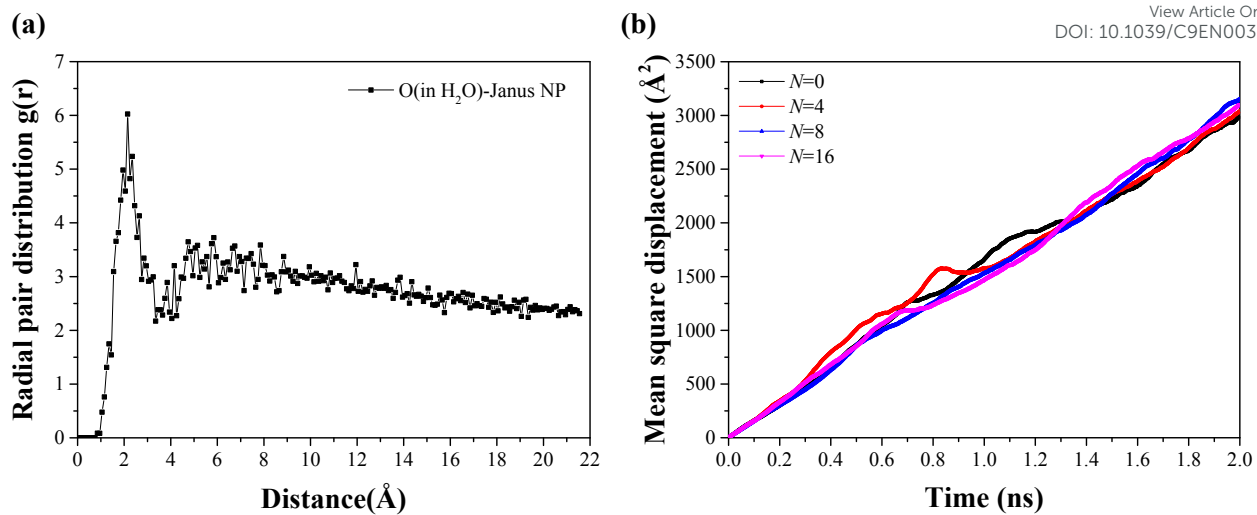
23

Figure 7 (a) Radial pair distribution function between oxygen atoms in water and the center of JNP; (b) Mean square displacement for nanofluids in confined channel.
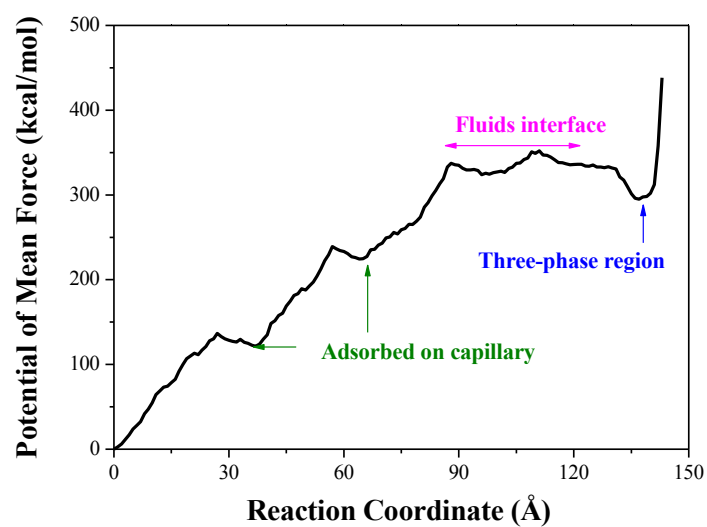
Figure 8 Potential of mean force (PMF) for JNP transporting from water to oil phase.
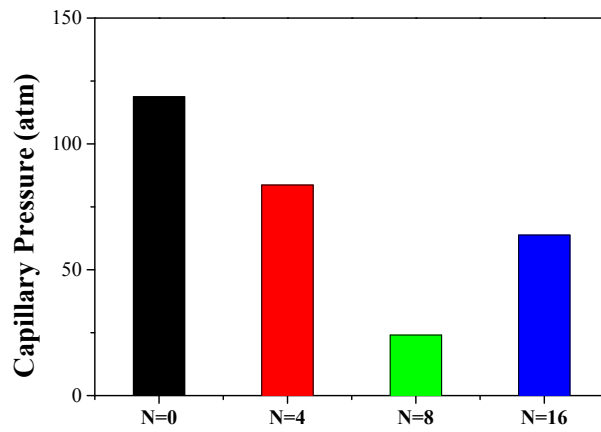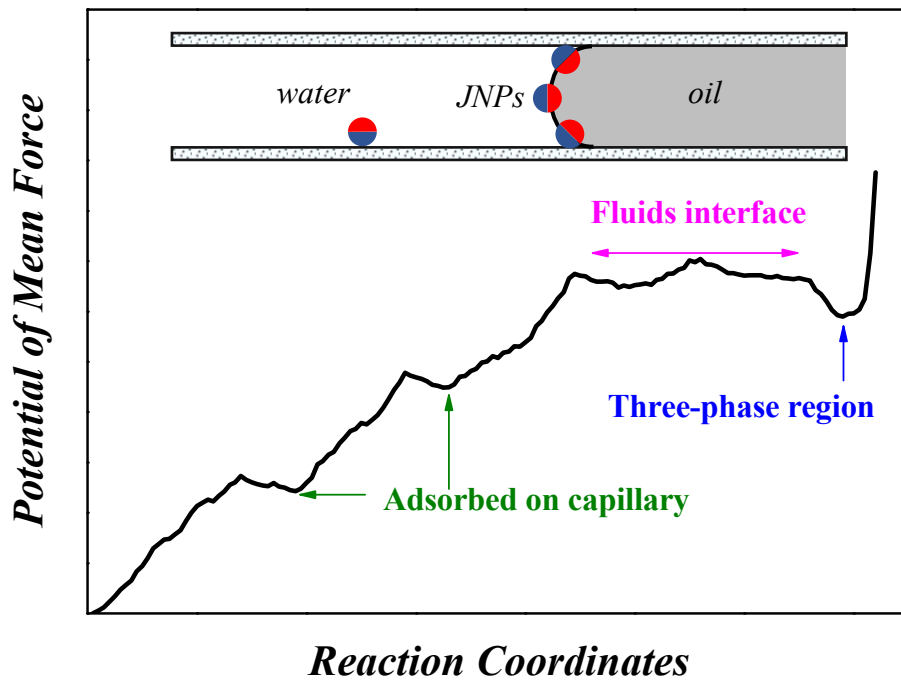
Figure 9 Calculated capillary pressure for nanofluids with different concentration of JNPs.

26

Graphics